

Modeling of a 6H-SiC MESFET for High-Power and High-Gain Applications

H. Arabshahi and M. Rezaee Rokn-Abadi

Department of Physics, Ferdowsi University of Mashhad, Mashhad, Iran

Abstract: A Monte Carlo simulation has been used to model steady state and transient electron transport in 6H-SiC field effect transistor. The simulated device geometries and doping are matched to the nominal parameters described for the experimental structures as closely as possible and the predicted 1-5 and transfer characteristics for the intrinsic devices show fair agreement with the available experimental data. Simulations of the effect of modulating, the gate bias have also been carried out to test the device response and derived the frequency bandwidth. Value of 90 ± 10 GHz has been derived for the intrinsic current gain cut-off frequency of the 6H-SiC MESFETs.

Key words: Steady-state, transient, cut-off frequency, frequency bandwidth, geometries, 6H-SiC

INTRODUCTION

6H-SiC is a wide band gap semiconductor ($E_g = 3$ eV) and therefore has a high breakdown field and low thermal generation rate. These properties combined with good thermal conductivity and stability make 6H-SiC an attractive material for high power, high temperature and radiation harsh environment electronic devices. Monte Carlo simulations predict a peak electron velocity of 3×10^7 cm sec⁻¹ and a saturation electron velocity of 1.3×10^7 cm sec⁻¹ (Mickevicius and Zhao, 1998; Trew and Shin, 1994). This makes possible high frequency operation of SiC devices. 6H-SiC is believed to be the most important SiC poly-type (in comparison to 3C or 4H-SiC) for high reliability power field effect transistor technology (Dohnke *et al.*, 1994; Agarwal, 1997; Joshi, 1995; Nilsson *et al.*, 1996) due to the higher than 4H-SiC conduction band offset with SiO₂. In this study, we analyze a Monte Carlo simulation which is used to model electron transport in hexagonal 6H-SiC MESFETs.

THE SIMULATION MODEL

Electron particles in the ensemble Monte Carlo simulation occupy non-parabolic ellipsoidal valleys in reciprocal space and obey Boltzmann statistics. Herring-Vogt transformations are used to map carrier momenta into spherical valleys when particles are drifted, scattered or cross heterojunctions (where care has been taken to ensure that the crystal momentum in the plane of the junction is conserved across the interface). The electric field equations are solved self-consistently with the electron transport using a finite difference method

(Walmsley and Abram, 1996) and the device grid potentials are updated at each ensemble drift time step (1 femto sec). Electrons in the bulk are scattered by ionized impurities and by bulk acoustic and non-polar optical phonon modes. Intervalley scattering by the absorption and emission of long wavelength acoustic and optic phonons have also been considered in the model. Model devices are built up as a series of joined rectangular regions with the electric field cell sizes matched along the join between each region (Arabshahi, 2006; Arabshahi and Ghasemian, 2006). Each region can consist of multiple layers of different alloy composition and doping/compensation density. The 6H-SiC MESFET can be described simply by three regions (Fig. 1), representing source and drain doping implants and a central region containing the supply layers. The field cell size used for the central region is 30 nm² (horizontal x vertical) but that in the high doped source and drain implants is finer (10 nm²).

Simulations of steady current characteristics have been carried out using 20000 electron particles; later simulations to derive the frequency response have required 50000 particles. Figure 1 shows a schematic of the modeled 6H-SiC MESFET. The overall device length is 2 μm in the x-direction and the device has a 0.2 μm gate length and 0.15 μm source and drain length. The source and drain have Ohmic contacts and gate is in Schottky contact in 1 eV to represent the contact potential at Au/Pt. The source and drain regions are doped to 2×10^{24} m⁻³ electron concentration and the top and down buffer layers are doped to 2×10^{23} m⁻³ and 5×10^{22} m⁻³ electron concentration, respectively. Subsequent to modeling the steady state characteristics, simulations of the effect of

modulating the gate bias have also been carried out in order to test the drain current response and drive the cut-off frequency corresponding to unit current gain. The frequency response was investigated by applying truncated sinc voltage pulse to both gate contacts of the 6H-SiC MESFET. The time dependence of the voltage signal is:

$$V_{gate}(t) = V_0 + V_{amplitude} \times \frac{\sin \omega(t - T/2)}{\omega(t - T/2)} \quad (1)$$

With:

$$\omega = 2\pi T/T_{mini}$$

Where:

- V_0 = Steady gate bias upon which the modulation signal is superimposed
- $V_{amplitude}$ = Peak voltage during the signal
- T = Duration of the signal
- T_{mini} = Duration of each minicycle within that signal

Table 1: Important parameters used in the simulations for 6H-SiC material

Parameters	6H-SiC
Density ρ (kgm^{-3})	3200
Longitudinal sound velocity v^s (ms^{-1})	1373
Low-frequency dielectric constant ϵ^s	9.7
High-frequency dielectric constant ϵ_∞	6.5
Acoustic deformation potential (eV)	15
Polar optical phonon energy (eV)	0.012
Γ -valley effective mass (m^*)	0.28
Γ -valley nonparabolicity (eV^{-1})	0.323

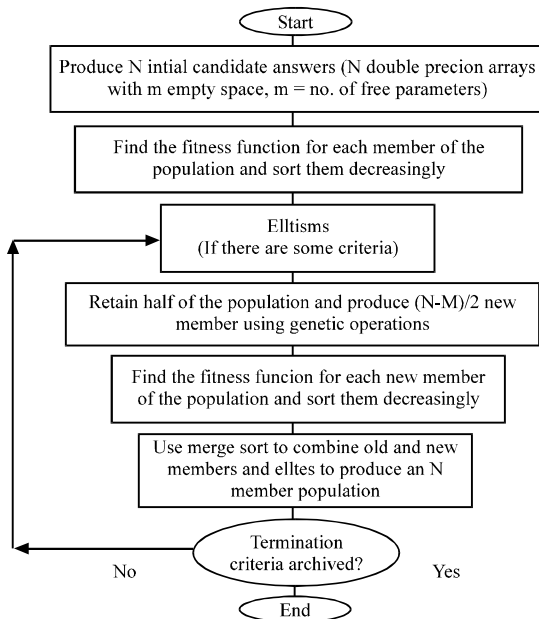


Fig. 1: The 2-dimensional model of 6H-SiC MESFET. The modeled structure is divided into three regions as indicated. Electron particles are initially distributed keeping all regions charge neutral. The location of the source and the drain implants and the top and back buffer layer are marked

In this instance 10 minicycles have been used. A 100 ps duration sinc-form pulse containing 10 minicycles has the specific advantage of providing a flat frequency spectrum up to 100 GHz with 10 GHz resolution. The material parameters used in the simulation are shown in Table 1.

SIMULATION RESULTS

Figure 2 shows the simulated drain current-voltage characteristic for the 6H-SiC MESFET with the gate voltage descending from -1 to -13 V in -2 intervals. The simulated characteristics at room temperature show good saturation behavior with a knee voltage around 20-30 V and a saturation drain current of about 1450 mA mm^{-1} for $V_{gs} = -1 \text{ V}$. The high drain current density is encouraging for the use of 6H-SiC for high power applications. It is also clear that the device is not completely pinched-off even at large negative gate bias ($V_{gs} = -13 \text{ V}$) which is due to strong electron injection into the buffer layer at high electric fields.

An increasing fraction of the drain current flows through the buffer as the drain voltage increases. Figure 3 and 4, respectively show the steady state Γ -valley band profile and the total electron density as a function of distance from the source when the drain-source potential drop is 20 V and the gate voltage is -1 V. Almost all the drain-source potential is dropped within the gate-drain region of the channel, leaving a flat potential profile near the source and drain. As electrons move towards the drain, they lose potential energy and gain sufficient kinetic energy to transfer to the upper conduction valleys where their drift velocity is reduced. Figure 4 shows the electron density through the device. The gate depletion region is clearly seen where the

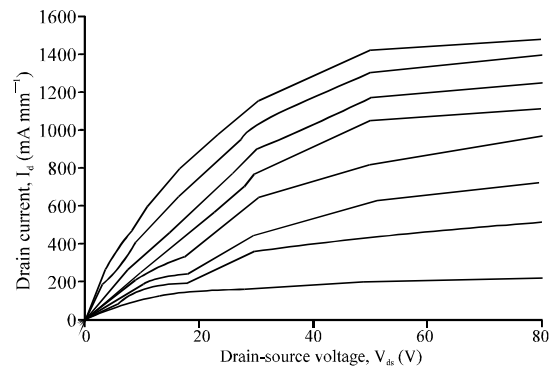


Fig. 2: Simulated current-voltage characteristics for the 6H-SiC MESFET at 300 K. The gate voltage ranges from -1 to -13 V in -2 V intervals. The knee voltage at around 20-30 V

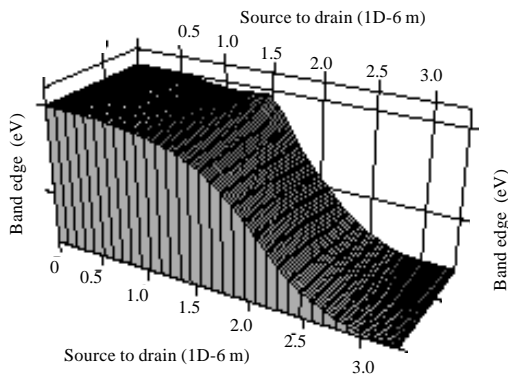


Fig. 3: Interpolated contour plot showing the steady state Γ -valley band profile through the simulated 6H-SiC MESFET at room temperature when the bias applied to the gate is -1 V and the drain-source bias is 20 V

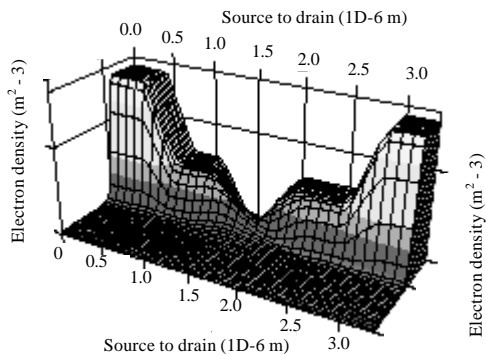


Fig. 4: Logarithmic plot indicating the electron density throughout the modeled region of the 6H-SiC MESFET when the bias applied to the gate is -1 V and the drain-source bias is 20 V

electron density is several orders of magnitude lower than it is near the source and drain. Figure 5a-c, respectively shows the sinc voltage signal applied to the gate, the drain current response and the gate current for the simulated 6H-SiC MESFET.

In Fig. 5a-c, the gate current (I_{gate}) is electric displacement, so resembles the derivative of the sinc voltage (V_{gate}). The gate current shown is the sum of the electric displacement, occurring at the left and right hand electrodes (Fig. 1).

The reproduction of the sinc pulse in the time dependence of the drain current is easy to discern, despite high frequency noise on the recorded currents which is a direct consequence of the motion of the finite number of electron particles across the field cell grid in the simulation. The current gain has been derived as a function of frequency by taking fast Fourier

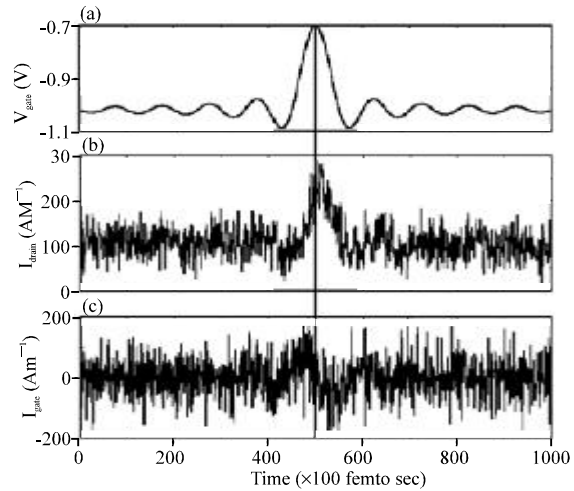


Fig. 5: The simulated frequency response of 6H-SiC MESFET to a sinc gate voltage pulse. From top to bottom, this figure shows the gate voltage (V_{gate}) as a function of time for a truncated pulse of duration 100 ps, the drain current response (I_{drain}) and the gate current (I_{gate}) which is electric displacement

transforms of the simulated drain and gate current signals then obtaining the ratios of the coefficients of the drain and gate current transforms. The calculated cut-off frequency for the simulated device is about 90 ± 10 GHz. If the data are extrapolated to the low frequency limit, the current gain is expected to be of the order of 20 dB.

CONCLUSION

A Monte Carlo simulation was used to model steady state and transient electron transport in a 6H-SiC metal semiconductor field effect transistor. The simulation results show that due to the high drain current density we can expect 6H-SiC devices have superior high power and high gain performance. The frequency response of the device has also been studied by applying a sinc pulse and sinusoidal signals at a range of frequencies to the gate.

Due to the high intrinsic cut-off frequency ($\approx 90 \pm 10$ GHz) the present results can also provide the useful advantages of 6H-SiC MESFET for high frequency performance.

ACKNOWLEDGEMENT

I would like to thank Maryam Gholvani for writing up the study.

REFERENCES

- Agarwal, A.K., 1997. Silicon carbide power device development. Proceedings of the 2nd International All Electric. Electronic Combat Vehicle Conference (AECV-II), June 8-12, Dearborn, MI. USA., pp: 13-19.
- Arabshahi, H. and M.H. Ghasemian, 2006. Influence of polarization charges and electron trapping in the buffer layer in wurtzite phase AlGa_N/Ga_N HFETs. *Modern Phys. Lett. B*, 20: 1397-1404.
- Arabshahi, H., 2006. Monte carlo simulations of electron transport in wurtzite phase gan mesfet including trapping effect. *Modern Phys. Lett. B*, 20: 787-794.
- Dohnke, K., R. Rupp, D. Peters, J. Volkl and D. Stephani, 1994. 6H-SiC field effect transistor for high temperature applications. Proceedings of the American Institute of Physics Conference (AIPCS'94), IOP Publishing, Bristol, UK., pp: 625-627.
- Joshi, R.P., 1995. Monte carlo calculations of the temperature- and field-dependent electron transport parameters for 4H-SiC. *J. Applied Phys.*, 78: 5518-5521.
- Mickevicius, R. and J.H. Zhao, 1998. Monte carlo study of electron transport. *J. Applied Phys.*, 83: 3161-3167.
- Nilsson, H.E., U. Sannemo and C.S. Petersson, 1996. Monte Carlo simulation of electron transport in 4H-SiC using a two-band model with multiple minima. *J. Applied Phys.*, 80: 3365-3369.
- Trew, R.J. and M.W. Shin, 1994. Wide bandgap semiconductor MESFETs for high temperature applications. Proceedings of the 3rd International Workshop on Integrated Nonlinear Microwave and Millimeterwave Circuits, Oct. 5-7, Duisburg, Germany, pp: 109-123.
- Walmsley, M. and R.A. Abram, 1996. A fast poisson solver for realistic semiconductor device structures. COMPEL: *Int. J. Comput. Math. Electr. Electron. Eng.*, 15: 31-51.